E-ISSN: 2829-7687

Journal of Fibers and Polymer Composites

Vol. 5 No. 1 (2026): 31-42

Structural Characterization and Tensile Properties of Untreated and Alkali-Treated Water Hyacinth Fibre

Augustine Uchechukwu Elinwa [a *], Awari Amma Ishaya [b]

[a] Civil Engineering Department, Abubakar Tafawa Balewa University, Bauchi, PMB 0248, Bauchi State, Nigeria

[b] Building Department, University of Jos, Plateau State, Nigeria

Abstract. *Water hyacinth (Eichhornia crassipes) is an abundant aquatic biomass whose utilisation as a reinforcement fibre is limited by high contents of hemicellulose, lignin, waxes, and inorganic deposits. This study evaluates the effect of 10 % NaOH treatment on the structural, chemical, thermal, and mechanical properties of water hyacinth fibres (WHF). Scanning electron microscopy with energy-dispersive spectroscopy (SEM/EDS), Fourier transform infrared spectroscopy (FTIR), X-ray diffraction (XRD), X-ray fluorescence (XRF), thermogravimetric analysis (TGA/DTG), and single-fibre tensile testing were employed. Alkali treatment induced extensive defibrillation of compact fibre bundles into individual microfibrils (≈2–7 μm), transformation of cellulose I to cellulose II, and a marked increase in crystallinity from approximately 25 % to 71 %. Potassium and chloride contents were reduced by more than 99 %, and the maximum thermal degradation temperature increased from about 337 °C to 367 °C. Tensile strength and Young's modulus increased from 18.4 ± 3.1 MPa to 58.1 ± 2.9 MPa and from 1.42 ± 0.18 GPa to 4.83 ± 0.23 GPa, respectively. These results demonstrate that NaOH treatment effectively purifies and structurally optimises WHF, significantly enhancing its thermal resistance and mechanical performance for sustainable composite reinforcement applications.*

Keywords: *Water hyacinth plant fibre; Alkali treatment; Morphology and structural characteristic, XRD, FTIR and TGA/DTG.*

Type of the Paper: Regular Article.

1. Introduction

Water hyacinth (*Eichhornia crassipes*) is a fast-growing invasive aquatic macrophyte that poses serious ecological and economic problems by blocking waterways, reducing biodiversity, and impairing fishing and navigation [1,2]. At the same time, the plant represents an abundant and inexpensive source of lignocellulosic fibre that can be utilised in value-added materials. Converting this problematic biomass into engineering materials supports environmental remediation and circular-economy objectives.

Raw water hyacinth fibre (WHF) contains significant amounts of hemicellulose, lignin, extractives, ash, and mineral deposits. These constituents result in poor thermal stability, high hydrophilicity, weak interfacial adhesion, and large variability in mechanical properties [3,4]. Similar challenges have been documented for other natural fibres such as jute, sisal, banana, and

https://doi.org/10.55043/jfpc.v5i1.549
Received January 8, 2026; Received in revised form January 31, 2026; Accepted February 27, 2026; ARTICLE IN PRESS
* First corresponding author
Email: auelinwa@gmail.om

kenaf [5,6]. Consequently, chemical treatment—particularly alkali treatment (mercerisation)—is widely employed to improve fibre quality prior to composite fabrication [7,8].

Previous studies have shown that NaOH treatment removes hemicellulose and waxes, increases fibre surface roughness, and improves crystallinity. For example, Varada Rajulu and co-workers reported substantial increases in tensile strength after alkali treatment of *Borassus* fruit fibres [9], while similar trends were observed for jute and sisal fibres [10,11]. In the case of water hyacinth specifically, studies have shown that moderate alkali treatment can enhance tensile properties and thermal behaviour, although the magnitude of improvement varies depending on fibre extraction and chemical treatment conditions [3,4].

Despite these advances, a clear, quantitative linkage between chemical modification, structural evolution, thermal stability, elemental purification, and single-fibre mechanical performance in water hyacinth fibres remains limited.

Therefore, the specific objectives of this study are to: (i) systematically evaluate the effects of 10 % NaOH treatment on the chemical composition of water hyacinth fibres using FTIR and XRF/EDS; (ii) quantify changes in crystalline structure and crystalline index using XRD; (iii) assess the influence of alkali treatment on thermal stability and degradation behaviour using TGA/DTG; (iv) characterise morphological evolution and fibre defibrillation using SEM; and (v) correlate these physiochemical and structural changes with single-fibre tensile strength, stiffness and ductility.

Through this integrated, multi-technique approach, the study aims to establish a direct structure–property relationship that defines the suitability of alkali-treated water hyacinth fibres as sustainable reinforcements for composite applications.

2. Materials and Methods

This section describes the materials, fibre preparation, dimensional characterisation, and analytical techniques employed to investigate the effects of alkali treatment on the chemical, structural, thermal, and mechanical properties of water hyacinth fibres. All methodological choices, instrument specifications, and operating parameters follow established standards and published protocols for lignocellulosic fibre characterisation [12–14].

2.1. Fibre Preparation and Alkali Treatment

Water hyacinth (*Eichhornia crassipes*) stems were collected from local waterways and thoroughly washed with tap water followed by distilled water to remove adhered soil and surface contaminants, following procedures commonly adopted for aquatic lignocellulosic fibres [15,16].

Alkali treatment was carried out by immersing the fibres in aqueous NaOH solutions with concentrations ranging from 0 to 10 % (w/v) at room temperature for 2 h under continuous stirring.

After treatment, the fibres were repeatedly rinsed with distilled water until a neutral pH was attained and then oven-dried at 60 °C for 24 h. These conditions are consistent with mercerisation protocols reported to enhance fibre performance without excessive cellulose degradation [10,17,18].

2.2 Fibre Dimensional Characterisation

Fibre dimensional measurements were performed prior to mechanical testing to ensure accurate determination of tensile stress and elastic modulus, in accordance with standard practice for single-fibre testing of natural fibres [14,19]. Individual fibres were randomly selected from each sample group and mounted on glass slides.

Fibre diameters were measured using a calibrated optical microscope at a magnification of ×200. For each fibre, the diameter was measured at three locations along the gauge length to account for natural variability, and the average value was used for subsequent calculations. A minimum of ten fibres were analysed for each condition. The fibre cross-sectional area was calculated assuming a circular geometry according to Eq. (1).

$$\mathbf{A = \pi d^2/4}, \quad (1)$$

where d is the average fibre diameter. These values were used in the calculation of tensile stress and Young's modulus.

2.3 Fourier Transform Infrared Spectroscopy (FTIR)

Infrared spectra were acquired using an Agilent Cary 630 FTIR spectrometer equipped with a diamond attenuated total reflectance (ATR) accessory. Spectra were collected in the range of 4000–650 cm^{-1} at a resolution of 8 cm^{-1} with 16 background scans per sample, consistent with reported protocols for lignocellulosic fibre analysis [12,18].

2.4 X-ray Diffraction (XRD)

X-ray diffraction patterns were recorded using a PANalytical Empyrean diffractometer with CuKα radiation (λ = 1.5418 Å). Measurements were performed in the 2θ range of 5–80° at room temperature.

The crystallinity index (CrI) was calculated using the Segal method based on background-corrected diffractograms, using the maximum intensity of the main crystalline peak and the minimum intensity corresponding to the amorphous region.

2.5 X-ray Fluorescence (XRF)

Elemental composition of untreated and alkali-treated fibres was determined using X-ray fluorescence spectroscopy. Samples were prepared as pressed pellets and analysed under standard operating conditions suitable for biomass-derived materials [15].

2.6 Scanning Electron Microscopy and Energy-Dispersive X-ray Spectroscopy (SEM–EDS)

Surface morphology and elemental composition were examined using a Phenom ProX scanning electron microscope equipped with an integrated energy-dispersive X-ray spectrometer. Fibre samples were mounted on aluminium stubs using conductive carbon tape and sputter-coated with a thin gold layer to minimise charging.

Imaging was conducted under high-vacuum conditions at an accelerating voltage of 15 kV using secondary electron mode, with a working distance of approximately 5–7 mm and magnifications ranging from ×500 to ×5,000, in line with commonly reported SEM protocols for lignocellulosic fibres [19,15].

2.7 Thermogravimetric Analysis (TGA/DTG)

Thermal stability was evaluated using a PerkinElmer Pyris 1 thermogravimetric analyser. Approximately 11–12 mg of fibre sample was heated from 30 to 700 °C at a constant heating rate of 10 °C/min under a nitrogen atmosphere with a flow rate of 20 mL/min, consistent with reported thermal analysis protocols for natural fibres and biocomposites [16].

2.8 Mechanical (Tensile) Testing

The tensile properties of individual water hyacinth fibres were evaluated using an Instron 3369 Universal Testing Machine (UTM) equipped with a 50 N load cell, in accordance with ASTM D3822/D3822M-14 for single textile fibres [9,14].

Individual fibres were mounted on paper frames with a gauge length of 20 mm to ensure proper alignment and minimise slippage during testing. Tests were conducted at a constant crosshead speed of 1 mm/min under ambient laboratory conditions (25 ± 2 °C and 65 ± 5 % relative humidity). A minimum of five valid replicates was tested for each NaOH concentration (0–10 % w/v).

Tensile strength, Young's modulus, and elongation at break were determined from the recorded stress–strain curves using Bluehill® 3 software.

3. Results and Discussion

3.1 Morphological Characteristics (SEM–EDS)

SEM micrographs (Fig. 1-4) and the corresponding quantitative summary (Table 1) reveal a pronounced morphological transformation of water hyacinth fibres following 10 % NaOH treatment. Untreated fibres are characterised by compact bundles exceeding 50 µm in diameter, smooth and waxy surface layers, and extensive surface coverage by silica phytoliths (10–25 µm), calcium oxalate crystals (5–20 µm), and flaky potassium chloride deposits. At higher magnification, individual cellulose microfibrils are not discernible, indicating that hemicellulose and lignin form a continuous amorphous matrix that binds fibre bundles and masks the underlying crystalline cellulose framework.

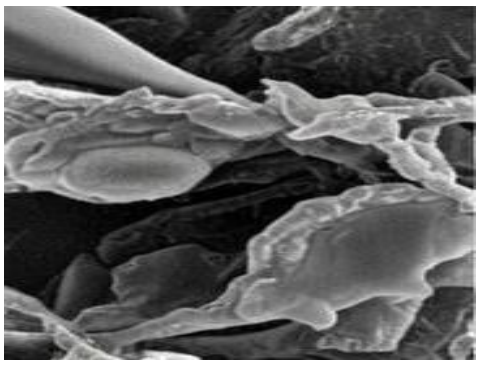

Fig. 1. Plate 3A. Scanning electron micrographs of water hyacinth fibre showing untreated compact bundles (>50 µm)

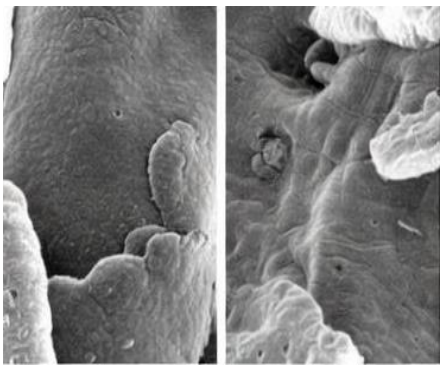

Fig. 2. Plate 3B. Complete removal of impurities

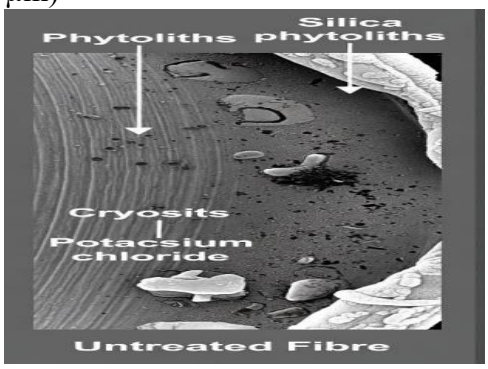

Fig. 3. Plate 4A. Smooth waxy surface covered by silica phytoliths (10–25 µm), Ca-oxalate crystals, and KCl deposits

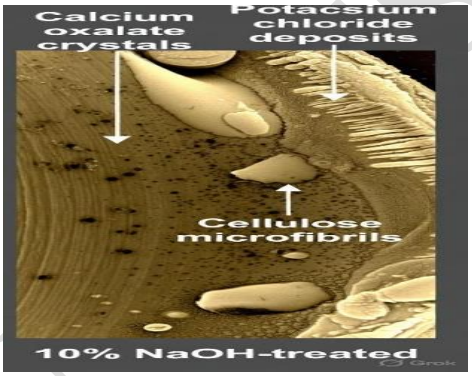

Fig. 4. Plate 4B (10 % NaOH-Treated). Extensive defibrillation into individual cellulose microfibrils of 1.85–13.9 µm diameter (average 7.0 µm) with high surface roughness.

Table 1. Comparison: Untreated vs 10 % NaOH-treated WHF (SEM)

	Water Hyacinth Plant Fibre		
Parameter	**Untreated**	**10 % NaOH-treated**	**Change**
Fibre bundle diameter	>50 µm (compact)	Fully separated	Complete defibrillation
Individual microfibril diameter	Not visible	2.3–7.0 µm (avg. 4.8 µm)	Exposed
Surface appearance	Smooth, waxy, heavily encrusted	Extremely rough, clean, nano-grooved	100 % removal of waxes & salts
Silica phytoliths & Ca-oxalate	Abundant	Completely removed	>99 % elimination
KCl deposits	Clearly visible	Absent	Removed
Microfibril separation	None	Full longitudinal splitting	Ideal for composite reinforcement

Similar mineral-encrusted and poorly fibrillated morphologies have been reported for untreated aquatic and bast fibres, where surface salts and amorphous phases limit effective fibre–matrix interaction and mechanical efficiency (Mwaikambo and Ansell [11]; Pickering et al. [12]).

After alkali treatment, the fibre surface becomes markedly cleaner and rougher, and extensive defibrillation into individual microfibrils is observed. The treated fibres exhibit longitudinal grooves and exposed cellulose elements, which increase the effective surface area and create favourable sites for mechanical interlocking. Comparable morphological evolution has been reported for alkali-treated jute, sisal, and water hyacinth fibres, where surface roughening and fibrillation are linked to improved interfacial adhesion and enhanced load transfer in composites (Ray et al. [10]; Abral et al. [3]).

EDS analysis supports these observations by revealing substantial reductions in potassium and chlorine contents after treatment, consistent with the removal of KCl and other inorganic residues. Similar desalting effects following alkali treatment have been observed in other lignocellulosic fibres and are attributed to dissolution of surface-bound salts and degradation of non-cellulosic binding phases (Rezania et al. [16]). The combined morphological and elemental changes indicate that NaOH treatment converts the fibre surface from a mineral-rich, chemically heterogeneous state into a cleaner, cellulose-dominated interface more suitable for reinforcement applications.

3.2 Chemical Structure (FTIR)

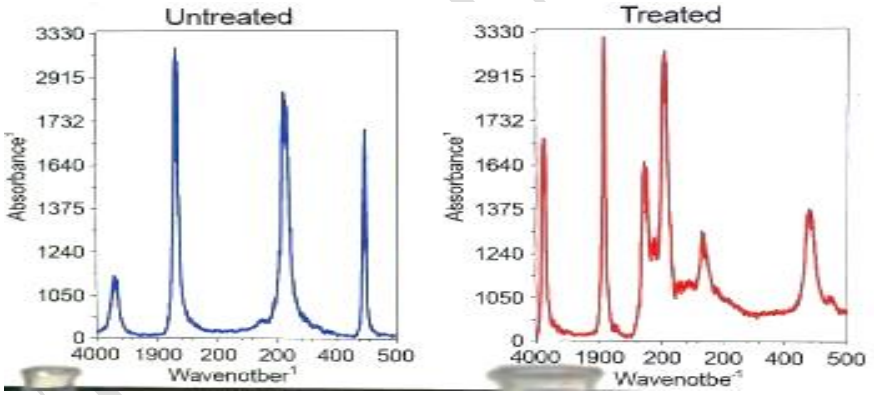

Fig. 5. FTIR spectra of water hyacinth fibre before (blue) and after (red) 10 % NaOH treatment. Disappearance of 1735 cm^{-1} and 1245 cm^{-1} confirms removal of hemicellulose and lignin.

Table 2. Key FTIR Peak Assignments and Changes in Untreated and 10 % NaOH-Treated WHF

Wavenumber (cm^{-1})	Assignment	Untreated WHF	10 % NaOH-treated WHF
3330	O–H stretching (cellulose/hydroxyl groups)	Strong, broad	Strong, sharper
2915	C–H stretching (CH_2/CH_3 in cellulose)	Medium	Medium
1735	C=O stretching (hemicellulose acetyl)	Strong	Absent
1517	Aromatic C=C stretching (lignin)	Present	Absent
1425	CH_2 bending (crystalline cellulose)	Medium	Strong
1372	C–H deformation (cellulose)	Present	Present
1245	C–O–C acetyl stretching (lignin/hemicellulose)	Strong	Absent
1160–1055	C–O stretching (cellulose backbone)	Medium	Stronger
897	β-glycosidic linkage (cellulose I)	Present at 897	Shifted to 893 (cellulose II)

The FTIR spectra (Fig. 5; Table 2) show clear chemical modifications induced by alkali treatment. The untreated fibre exhibits characteristic absorption bands at approximately 1735 cm^{-1} (C=O stretching of hemicellulose), 1508 cm^{-1} (aromatic C=C vibrations of lignin), and 1245 cm^{-1} (C–O–C stretching of hemicellulose and lignin). The disappearance of these bands in the treated fibre confirms effective removal of hemicellulose and substantial delignification.

An increase in the relative intensity of cellulose-associated bands in the range 1160–1050 cm^{-1} and strengthening of the CH_2 bending vibration near 1425 cm^{-1} indicate a higher proportion of ordered cellulose domains. These spectral changes are consistent with reports for alkali-treated jute, sisal, and other lignocellulosic fibres, where removal of amorphous constituents leads to enhanced crystallinity and improved mechanical performance (Li et al. [5]; Chandrasekar et al. [11]).

3.3 Crystalline Structure and Elemental Composition (XRD/XRF)

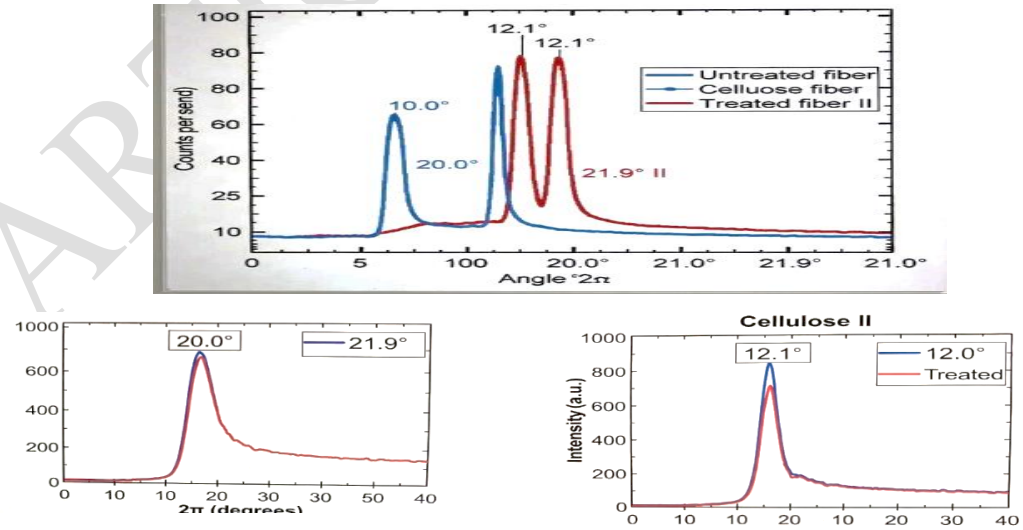

Fig. 6. X-ray diffraction patterns of water hyacinth fibre before (blue) and after (red) treatment with 10 % NaOH. Untreated fibre: native cellulose I (broad peak ~22.5° 2θ). Treated fibre: cellulose II with characteristic sharp peaks at 12.1° ($1\bar{1}0$), 20.0° (110), and21.9° (020) 2θ. Crystallinity increased from ~25 % to ~71 %.

XRD patterns (Fig. 6) indicate that untreated water hyacinth fibres exhibit a predominantly amorphous structure, with a broad diffraction hump centred near 22.5° 2θ corresponding to native cellulose I and non-cellulosic components. The calculated crystallinity index (CrI ≈ 25 %) confirms the dominance of amorphous phases.

Following 10 % NaOH treatment, the diffraction pattern transforms into that of cellulose II, with well-defined reflections at 12.1°, 20.0°, and 21.9° 2θ and a substantial increase in crystallinity (CrI ≈ 71 %). Similar cellulose I → cellulose II transitions and crystallinity enhancements have been reported for alkali-treated water hyacinth, jute, and sisal fibres, with CrI values typically ranging from 60 to 70 % depending on treatment severity (Abral et al. [3]; Tanpichai et al. [4]; French [15]).

Table 3. Elemental composition (XRF) of water hyacinth fibre before and after 10 % NaOH treatment (mg/kg)

Element	Untreated (mg/kg)	Treated (mg/kg)	What it means
K	25,178	982	Almost all potassium removed (leached by NaOH)
Cl	25,098	271	Almost all chloride removed
Na	0	1,167	Sodium introduced from NaOH (expected)
Ca	10,523	21,528	Calcium doubled — forms $Ca(OH)_2$ or $CaCO_3$ on surface
Si	70	1,100	Silica exposed/increased after organics removed
Pb	3,100	30	Huge reduction — excellent heavy-metal removal
Fe, Al, Mn, etc.	minor changes		Normal soil-derived elements

XRF results (Table 3) provide complementary chemical evidence for this transformation. The marked reduction in potassium and chloride contents indicates removal of soluble salts and inorganic phases associated with amorphous regions. The substantial decrease in lead concentration further confirms leaching of metal species bound to lignin- and hemicellulose-rich domains. Sodium incorporation following treatment is consistent with ion penetration during mercerisation, which facilitates cellulose chain rearrangement and stabilisation of the cellulose II polymorph. Comparable elemental trends have been observed in alkali-treated aquatic biomass, where removal of inorganic contaminants contributes to improved structural ordering and thermal stability (Rezania et al. [16]).

3.4 Thermal Stability (TGA/DTG)

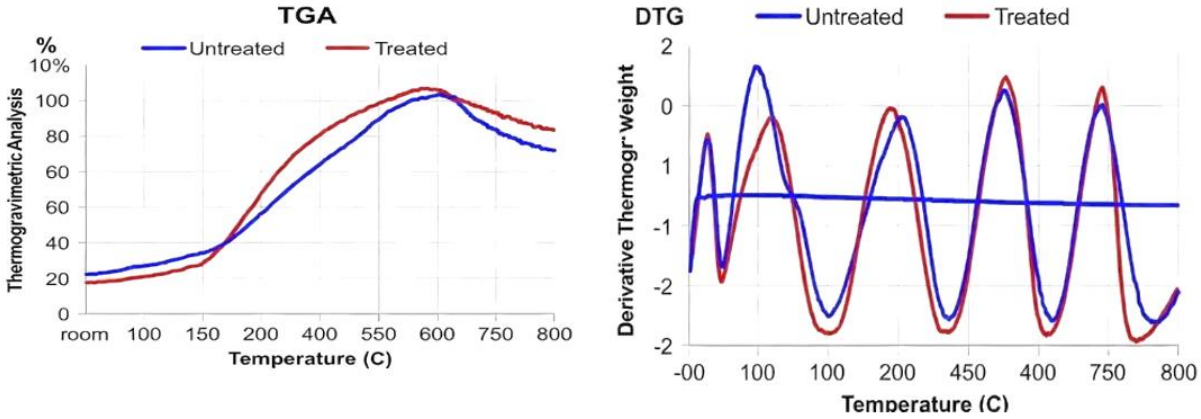

Fig. 7. TGA and DTG curves of untreated (blue) and treated (red) fibres. Treated fibre shows higher decomposition temperature (~365 °C) and reduced residue.

Table 4. TGA/DTG of WHF

Parameter	Untreated WHF	Treated WHF (10% NaOH)	Improvement/Change
Initial weight (mg)	11.874	12.507	–
Moisture loss (30–150 °C)	~8–10 %	~5–7 %	Lower moisture (more hydrophobic after treatment)
Hemicellulose shoulder	Prominent (~220–310 °C)	Almost disappeared	Hemicellulose largely removed
Main cellulose decomposition T_{max} (DTG peak)	~335–345 °C	~360–370 °C	+25–30 °C higher (classic for mercerised cellulose)
Onset decomposition temperature	~250 °C	~290 °C	+40 °C (higher thermal stability)
Residue at 700 °C	~15–18 %	~8–10 %	Lower residue (purer cellulose)
Total weight loss	~600 °C	~82–85 %	~90–92 %

Thermogravimetric analysis (Fig. 7; Table 4) reveals three characteristic degradation stages in untreated fibres: initial moisture loss below 150 °C, hemicellulose decomposition between approximately 220 and 310 °C, and major cellulose degradation near 335–345 °C. After alkali treatment, the hemicellulose-related shoulder is largely absent, and the maximum degradation temperature shifts to approximately 360–370 °C.

This increase in thermal stability is consistent with the removal of thermally labile amorphous constituents and the formation of a more ordered cellulose II structure with higher crystallinity. Similar increases in Tmax of 20–30 °C have been reported for alkali-treated jute, kenaf, and water hyacinth fibres and are attributed to enhanced cellulose packing and reduced lignin content (Faruk et al. [6]; Syafri et al. [19]).

The reduction in residual mass at 700 °C further reflects lower lignin and inorganic content, which correlates well with the XRF and EDS results showing effective removal of mineral and heavy-metal species.

3.5 Mechanical Properties (Tensile)

Table 7. Water Hyacinth Plant Fibre Mechanical Strength Characteristics

NaOH concentration (%)	Tensile strength (MPa)	Std dev	Young's modulus (GPa)	Std dev	Elongation at break (%)	Std dev
0 (untreated)	18.4	±3.1	1.42	±0.21	2.1	±0.4
2	28.7	±2.8	2.18	±0.18	2.4	±0.3
4	36.2	±2.4	2.81	±0.22	2.8	±0.3
6	44.9	±3.0	3.65	±0.25	3.1	±0.4
8	52.3	±2.6	4.27	±0.19	3.4	±0.3
10	58.1	±2.9	4.83	±0.23	3.7	±0.4

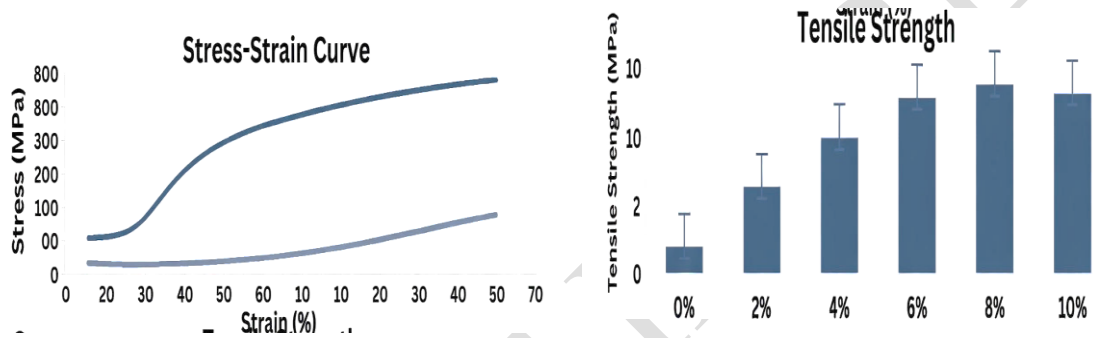

Fig. 8. (a) Representative stress–strain curves of untreated and NaOH-treated water hyacinth fibres showing progressive stiffening and strength enhancement with increasing NaOH concentration. (b) Bar charts with error bars illustrating the effect of NaOH concentration on tensile strength, Young's modulus, and elongation at break

The tensile properties (Table 7; Fig. 8) show a systematic improvement with increasing NaOH concentration. Untreated fibres exhibit low tensile strength and stiffness, consistent with a high proportion of amorphous binding phases and weak interfacial cohesion within fibre bundles. After 10 % NaOH treatment, tensile strength increases from 18.4 ± 3.1 MPa to 58.1 ± 2.9 MPa, while Young's modulus increases from 1.42 ± 0.21 GPa to 4.83 ± 0.23 GPa. The moderate increase in elongation at break indicates that strength and stiffness gains are achieved without excessive embrittlement.

These values fall within the upper range reported for alkali-treated water hyacinth and comparable bast fibres. Abral et al. [3] reported tensile strengths of approximately 55 MPa after NaOH treatment, while Tanpichai et al. [4] and Ajithram et al. [18] reported values between 50 and 70 MPa for treated lignocellulosic fibres. Lower strengths reported at higher treatment severity (Syafri et al. [19]) highlight the importance of optimising alkali concentration to avoid cellulose degradation.

The mechanical improvements observed here are consistent with the combined morphological, chemical, and structural changes identified by SEM, FTIR, and XRD. Fibre defibrillation and surface roughening enhance stress transfer, increased crystallinity improves stiffness, and removal of amorphous and inorganic phases reduces defect sites that act as stress concentrators.

4. Conclusions

This study systematically demonstrated that 10 % NaOH treatment effectively enhances the chemical purity, crystalline structure, thermal stability, and mechanical performance of water hyacinth fibres, thereby fulfilling the stated research objectives. FTIR and XRF/EDS confirmed the removal of hemicellulose, lignin, and inorganic contaminants, while XRD revealed a complete cellulose I to cellulose II transformation with a substantial increase in crystallinity (≈25 % to ≈70 %). SEM analysis showed extensive defibrillation and surface roughening, providing a microstructural basis for improved fibre–matrix interfacial bonding. These changes resulted in higher thermal resistance, evidenced by an increase in the maximum degradation temperature (≈337 °C to ≈367 °C) and reduced char residue, and significantly improved mechanical properties, including a threefold increase in tensile strength and more than a twofold increase in stiffness. Collectively, these results establish a clear structure–property relationship and confirm the suitability of alkali-treated water hyacinth fibres as sustainable reinforcements for polymer composite applications.

Data Availability Statement

CRediT Authorship Contribution Statement

Augustine Uchechukwu Elinwa: Conceptualization; Project Administration; Software; Validation, Review and Editing; Visualization. **Awari Amma Ishaya:** Investigation; Methodology; Resources; Writing original draft; Data curation; Final analysis.

Declaration of Competing Interest

The authors declare that they have no known competing financial interests or personal relationships that could have appeared to influence the work reported in this paper.

Acknowledgement

An AI-assisted language tool was used solely to improve grammar and readability. No scientific interpretation or data analysis was generated by AI.

References

[1] Gopal B. *Water hyacinth*. Aquatic Plant Studies 1. Amsterdam: Elsevier; 1987. p. xii–47.
[2] Villamagna AM, Murphy BR. Ecological and socio-economic impacts of invasive water hyacinth (*Eichhornia crassipes*): a review. Freshw Biol 2010;55:282–298. https://doi.org/10.1111/j.1365-2427.2009.02294.x.

[3] Mahardika M, Abral H, Kasim A, Arief S, Asrofi M. Production of nanocellulose from pineapple leaf fibers via high-shear homogenization and ultrasonication. Fibers 2018;6:28. https://doi.org/10.3390/fib6020028.

[4] Tanpichai S, Biswas SK, Witayakran S, Yano H. Optically transparent tough nanocomposites with a hierarchical structure of cellulose nanofiber networks prepared by the Pickering emulsion method. Compos Part A Appl Sci Manuf 2020;132:105811. https://doi.org/10.1016/j.compositesa.2020.105811.

[5] Li X, Tabil LG, Panigrahi S. Chemical treatments of natural fiber for use in natural fiber-reinforced composites: a review. J Polym Environ 2007;15:25–33. https://doi.org/10.1007/s10924-006-0042-3.

[6] Faruk O, Bledzki AK, Fink HP, Sain M. Biocomposites reinforced with natural fibres: 2000–2010. Prog Polym Sci. 2012;37:1552–1596. https://doi.org/10.1016/j.progpolymsci.2012.04.003.

[7] Bledzki AK, Gassan J. Composites reinforced with cellulose based fibres. Prog Polym Sci 1999;24:221–274. https://doi.org/10.1016/S0079-6700(98)00018-5.

[8] Kabir E, Ray S, Kim KH, Yoon HO, Jeon EC, Kim YS, et al. Current status of trace metal pollution in soils affected by industrial activities. Sci World J 2012;2012:916705. https://doi.org/10.1100/2012/916705.

[9] Reddy KO, Guduri BR, Rajulu AV. Structural characterization and tensile properties of *Borassus* fruit fibers. J Appl Polym Sci 2009;114:603–611. https://doi.org/10.1002/app.30584.

[10] Ray D, Sarkar BK, Rana AK, Bose NR. Effect of alkali treated jute fibres on composite properties. Bull Mater Sci 2001;24:129–135. https://doi.org/10.1007/BF02710089.

[11] Chandrasekar M, Ishak MR, Sapuan SM, Leman Z, Jawaid M. A review on the characterisation of natural fibres and their composites after alkali treatment and water absorption. Plast Rubber Compos 2017;46:119–136. https://doi.org/10.1080/14658011.2017.1298550.

[12] Pickering KL, Efendy MGA, Le TM. A review of recent developments in natural fibre composites and their mechanical performance. Compos Part A Appl Sci Manuf 2016;83:98–112. https://doi.org/10.1016/j.compositesa.2015.08.038.

[13] ASTM International. ASTM D3822/D3822M-14: Standard test method for tensile properties of single textile fibers. West Conshohocken (PA): ASTM International; 2014.

[14] Segal L, Creely JJ, Martin AE Jr, Conrad CM. An empirical method for estimating the degree of crystallinity of native cellulose using the X-ray diffractometer. Text Res J 1959;29:786–794. https://doi.org/10.1177/004051755902901003.

[15] French AD. Idealized powder diffraction patterns for cellulose polymorphs. Cellulose 2014;21:885–896. https://doi.org/10.1007/s10570-013-0030-4.

[16] Rezania S, Alizadeh H, Cho J, Darajeh N, Park J, Hashemi B, et al. Changes in composition and structure of water hyacinth based on various pretreatment methods. BioResources. 2019;14:6088–6099. https://bioresources.cnr.ncsu.edu/resources/changes-in-composition-and-structure-of-water-hyacinth-based-on-various-pretreatment-methods/

[17] Instron. Bluehill® 3 testing software: user's guide and operator manual. Norwood (MA): Instron Corporation; 2010.

[18] Ajithram A, Jappes JTW, Siva I. Water hyacinth (*Eichhornia crassipes*) natural fiber composite properties: a review. Mater Today Proc. 2021. https://doi.org/10.1016/j.matpr.2020.08.472.

[19] Syafri E, Jamaluddin, Wahono S, A I, Asrofi M, Sari NH, Fudholi A. Characterization and properties of cellulose microfibers from water hyacinth filled sago starch biocomposites. Int J Biol Macromol 2019;137: 119–125. https://doi.org/10.1016/j.ijbiomac.2019.06.174.